100-Gb/s undersea transmission with high spectral efficiency using pre-filtered QPSK modulation format

(Invited Paper)

J.-X. Cai*, Y. Cai, C. R. Davidson, D. G. Foursa, A. Lucero, O. Sinkin, W. Patterson, A. Pilipetskii, G. Mohs, and Neal S. Bergano

Tyco Electronics Subsea Communications LLC ("TE SubCom" formerly known as Tyco Telecommunications (US) Inc.), 250 Industrial Way West, Eatontown, NJ 07724, USA

**E-mail: jcai@subcom.com*

Received June 12, 2010

We provide a review of our recent 100-Gb/s, high spectral efficiency (SE) experiment targeting transoceanic and regional undersea transmission distances. We demonstrated that simple pre-filtering at the transmitter together with a maximum *a posteriori* probability (MAP) detection algorithm can significantly improve SE. We transmitted 96×100-Gb/s pre-filtered polarization division multiplexed return-to-zero quadrature phase shift keyed (PDM-RZ-QPSK) channels with 300% SE over 10608 km using 52-km spans of 150-μm^2 fiber and simple single-stage erbium-doped fiber amplifiers (EDFAs). We also achieved 400% SE over 4368 km using similar techniques.

OCIS codes: 060.2330, 060.1660, 060.4510.
doi: 10.3788/COL20100809.0831.

1. Introduction

High spectral efficiency (SE), a desirable metric in all optical communications systems, is particularly challenging for transoceanic cable systems. The new paradigm of digital coherent receivers has enabled several impressive demonstrations. In 2009, we have seen transoceanic transmission demonstrations with 200% SE using the single-carrier polarization division multiplexing-quadrature phase shift keying (PDM-QPSK) modulation format[1,2] or the two-carrier PDM-QPSK modulation format[3]. Further SE enhancement (∼360%) was demonstrated with more elaborate PDM/orthogonal frequency division multiplexing (OFDM) techniques[4]. For all the aforementioned demonstrations, either Raman assisted erbium-doped fiber amplifiers (EDFAs) or pure Raman amplification was used to boost the received optical signal-to-noise ratio (OSNR) for the 100-Gb/s signals.

In our work, we transmitted 96×112-Gb/s pre-filtered PDM-RZ-QPSK (RZ: return-to-zero) channels over a 10608 km path constructed with an amplifier chain consisting of single-stage EDFAs and 150-μm^2 large effective area fiber[5]. The 300% SE was achieved with >10 dB Q-factor for all 96 channels. In addition, we achieved 400% SE over 4368 km also using pre-filtered PDM-RZ-QPSK. Both results were accomplished without differential decoding. The aggressive pre-filtering required for both demonstrations created significant back-to-back inter-symbol-interference (ISI) penalty which produces a more complex signal constellation and can also be interpreted as memory in the modulation format. We have developed a suite of algorithms to take advantage of the "memory" produced by pre-filtering to mitigate the linear ISI penalty associated with the tight filtering. We showed that > 400% SE is achievable using PDM-QPSK transmission.

2. Experimental setup

Figure 1 shows a schematic of our transmitter setup. We electrically generate four binary 28-Gb/s signals (I, $\overline{\text{I}}$ and Q, $\overline{\text{Q}}$ with pseudo-random bit sequence (PRBS) length 2^{23}–1) by multiplexing 14-Gb/s data streams from a four-channel pulse pattern generator (PPG). The 28-Gb/s streams are used in pairs for the in-phase (I) and quadrature (Q) ports of two QPSK modulators to generate two optical QPSK signals at 28 Gbaud or equivalently 56 Gb/s. After RZ pulse carving, each of the two optical signals is then split into two equal paths. One path is delayed with respect to the other to de-correlate the data patterns. The two data paths are then orthogonally recombined using a polarization beam combiner (PBC), resulting in two 112-Gb/s PDM-RZ-QPSK signals.

Each of the two QPSK modulators imparts its data onto a comb of wavelengths to generate two rails of odd and even channels. The two rails are pre-filtered and combined with cascaded 33-GHz or cascaded 25-GHz optical interleaving filters for 300% or 400% SE, respectively. Each rail consists of 48 distributed feedback (DFB) lasers and 4 tunable external cavity lasers (ECLs) with 1-pm resolution. The eight ECLs are tuned to a contiguous set of channels and the corresponding DFB lasers are disabled for the bit error measurements. This process is repeated and the ECLs are tuned across the band until all 96 channels are measured. All 96 channels are modulated in a similar fashion at all times. We also experimentally confirmed that a de-correlated 4-rail transmitter setup performed very similar to the 2-rail setup shown in Fig. 1 for 25-GHz channel spacing.

The 624-km circulating loop test-bed (Fig. 2) consists of twelve 52-km spans using a large effective area fiber with $A_{\text{eff}} \approx 150$ μm^2, mid-band chromatic dispersion ≈ 20.6 ps/(nm·km), and attenuation ≈ 0.183 dB/km. Each

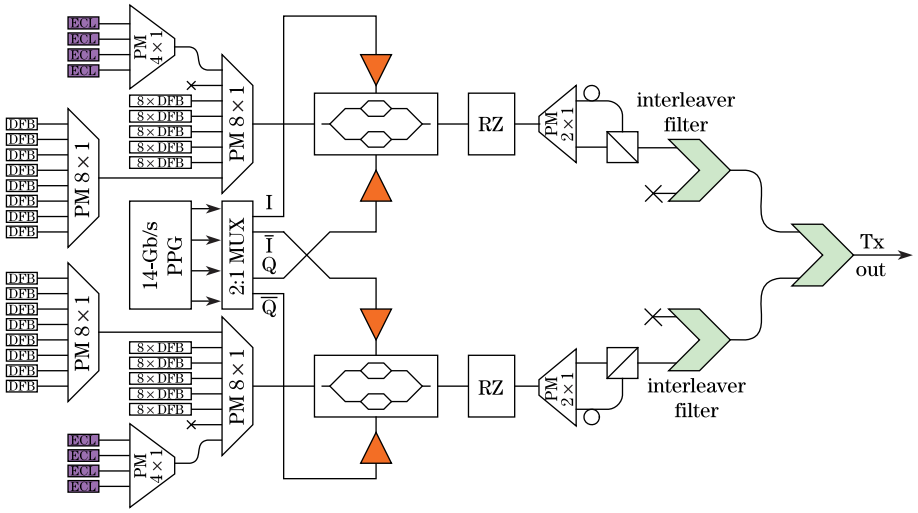

Fig. 1. 112-Gb/s PDM-RZ-QPSK transmitter. PM: polarization maintaining; MUX: multiplexer; Tx: transmitter.

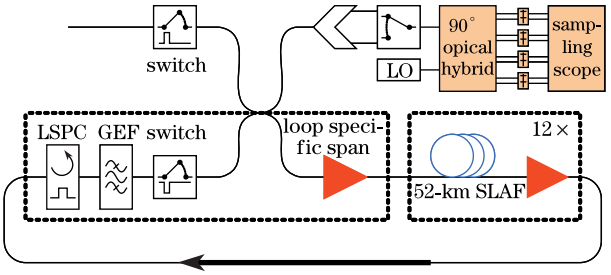

Fig. 2. Circulating loop test-bed and 112-Gb/s PDM-RZ-QPSK receiver. LSPC: loop synchronous polarization controller. GEF: gain equalized filter; LO: local oscillator; LAF: large area fiber.

span is equipped with a single-stage EDFA with 16-dBm output power and gain equalized to 26-nm bandwidth. The loop specific span contains a loop synchronous polarization controller (LSPC)[6] and a gain equalization filter to compensate residual loop gain error. The average polarization mode disperision (PMD) of the loop is 1.7 ps. No pre/post or in-line optical dispersion compensation was used in this experiment.

Our digital coherent receiver (Fig. 2) consists of cascaded interleaver filters (33 and 67 GHz or 25 and 50 GHz) followed by a tunable band-pass filter to demultiplex the channels and a polarization diversity 90° optical hybrid followed by four balanced detectors[7]. The electrical signals from the detectors are recorded using a digital sampling scope with 16-GHz analog bandwidth and 50-GS/s sampling rate. The recorded electrical signals were processed off-line with a computer.

3. Coherent receiver algorithms and ISI reduction

We performed the necessary digital signal processing off-line. After waveform recovery and alignment, dispersion compensation was performed digitally in the Fourier domain. The resulting waveform was then re-sampled at 2 samples/symbol with the recovered clock. A constant modulus algorithm (CMA) was used for polarization tracking and PMD compensation. Carrier phase estimation (CPE) was subsequently applied using the Viterbi-Viterbi algorithm[8]. The aggressive pre-filtering used to suppress wavelength division multiplexing (WDM) crosstalk also resulted in significant intra-channel ISI penalty. This pre-filtering penalty was compensated using a maximum *a posteriori* probability (MAP) detection algorithm[9].

Figure 3 shows transmission performance versus transmitter pre-emphasis for 3 different detection algorithms (Ch50 after 10608 km with 300% SE). In order to capture the full impact of linear and nonlinear interactions between neighboring channels, the power of eight contiguous channels was simultaneously changed (Ch50 being the 6th in the group of 8). QPSK shows better performance than differential coding QPSK (DCQPSK) similar to results in Ref. [10]. The results also show that MAP detection can recover up to ∼2 dB of ISI penalty at 300% SE.

4. 100-Gb/s transmission over 10608 km with 300% SE using pre-filtered QPSK

The 96×112-Gb/s WDM signals were launched into the test-bed without any individual channel power pre-emphasis. After 10608-km transmission (17 loops), the average received OSNR in 1-nm resolution bandwidth (RBW) was 6.7 dB, and the OSNR difference over the operating range was ∼ 2 dB, as shown in Fig. 4.

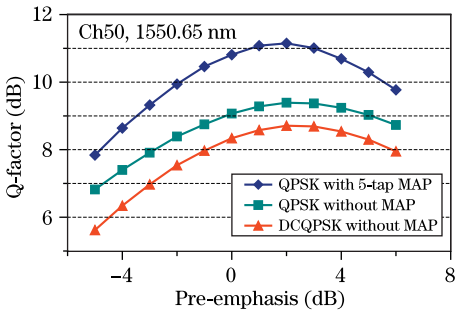

Fig. 3. Q-factor versus transmitter pre-emphasis after 10608 km (300% SE) with three different detection schemes.

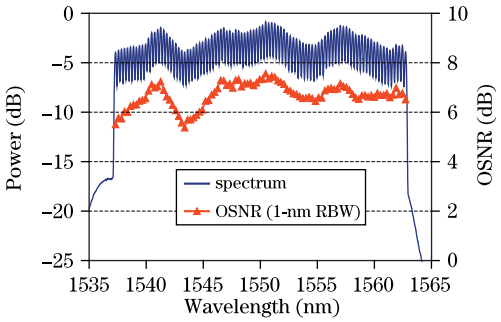

Fig. 4. Optical spectrum and OSNR (in 1-nm RBW) after 10608-km transmission.

The bit error rate (BER) of each channel was decoded from five sets of data with 2M samples each (22.4 Mb/ch). Figure 5 shows the Q-factor calculated from the average BER of the 5 data sets for each channel, together with the Q-factor of the two orthogonal polarizations. The average Q-factor for all channels (totally 2150 Mb of data decoded) was 10.7 dB, and the Q-factor of the worst channel was >10.1 dB. The Q-factor difference between the two polarizations of a particular channel was attributed to polarization dependent loss (PDL), and we observed up to 1.3-dB Q-factor difference between the two orthogonal polarizations. Even though the OSNR of Ch50 (Fig. 4) was close to the highest among all 96 channels, the operating power for this channel was still ~1 dB less than the optimum channel power as shown in the power sweep measurements (Fig. 3). Therefore, the performance of all channels could be further improved with increased EDFA output power. Figure 5 also shows the forward error correction (FEC) threshold (8.2 dB) for a 7% continuously-interleaved BCH code[11]. Compared with this FEC, all channels had ~2-dB average FEC margin.

In these experiments, we did not observe any cycle slips after decoding more than 2150 Mb at the 10608-km transmission distance. We estimate that the probability of cycle slips in our experiments was less than 10^{-8} with more than 99% confidence level, which is sufficiently low to be easily mitigated using digital signal processing (DSP), see for example Ref. [12]. A loop synchronous polarization controller was used to ensure that time-varying PDL and PMD were included in all measurements.

5. Pre-filtered QPSK to achieve 400% SE

To further explore the benefit of our MAP detection and CMA algorithms, we increased the SE to 400% by reducing the channel spacing to 25 GHz for the 28-Gbaud signals. All 33-GHz/67-GHz optical interleaving filters were replaced by 25-GHz/50-GHz optical interleaving filters. Figure 6 compares the optical spectrum of a single-channel RZ-QPSK signal, a single-channel NRZ-QPSK (NRZ: non-return-to-zero) signal, pre-filtered RZ-QPSK signals at 50-GHz channel spacing with 25-GHz optical interleaving filters, and pre-filtered RZ-QPSK signals with 25-GHz spacing. The aggressive optical pre-filtering effectively removed crosstalk from neighboring channels, as shown in Fig. 6. The spectrum of the pre-filtered RZ-QPSK is even narrower than that of NRZ-QPSK signal.

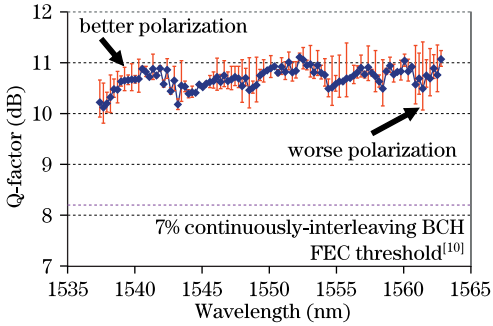

Fig. 5. Q-factor after 10608 km (300% SE).

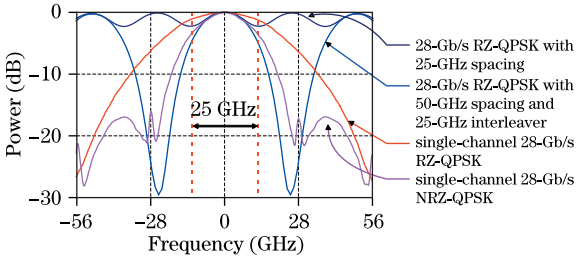

Fig. 6. Optical spectrum for RZ-QPSK, NRZ-QPSK, and pre-filtered QPSK.

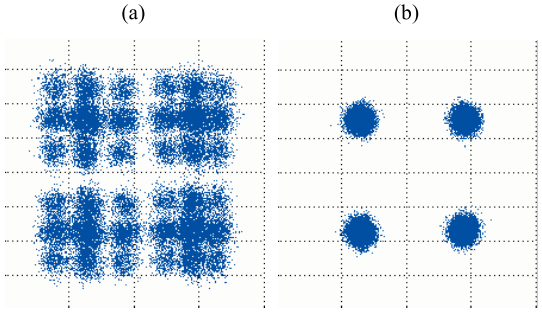

Fig. 7. 25-GHz pre-filtered 112-Gb/s RZ-QPSK shows complex constellation (for one polarization and without two immediate neighbor channels); (b) MAP detection algorithm recovers the constellation back to that of a typical QPSK signal.

While effectively limiting the crosstalk from neighboring channels, the aggressive pre-filtering also dramatically increased intra-channel ISI and hence created correlation (i.e., memory) between symbols. It was shown in Ref. [13] that a joint-statistics sequence detection scheme can effectively reverse the pre-filtering induced ISI penalty in a non-coherent on-off keying (OOK) system. The pre-filtering induced correlation can be seen in the constellation diagram as shown in Fig. 7(a) (for one polarization and without two immediate neighbor channels), where a single point in the typical QPSK constellation is transformed or converted into nine points. This four-group 3×3 or 4×(3×3) constellation is caused by the correlation between a symbol and its two nearest neighbors of the QPSK signal. Significant penalty is inevitable if only a single symbol detection algorithm is used. On the other hand, our MAP algorithm is able to take advantage of the ISI induced memory in the channel with a detection scheme based on multiple symbols. The joint detection reduces the penalty from over-filtering where the crosstalk from neighboring channels is small[14]. With the MAP detection algorithm, the ISI-heavy 4×(3×3) constellation

Table 1. Q-Factors with Different Conditions and Detection Schemes (10-dB OSNR)

Q-Factor with 10 dB OSNR in 1-nm RBW		QPSK	QPSK with 5-Tap MAP	MAP Benefit
Q_{SC}	Single Channel	15 (Extrapolated)		
$Q_{wo\_neighbor}$	28on25 without Neighbors	5.7	12.8	7.1
$Q_{w\_neighbor}$	28on25 with Neighbors	5.2	11.4	6.2
Q_{SC}–$Q_{wo\_neighbor}$	Filtering Penalty	9.3	2.2	
$Q_{wo\_neighbor}$–$Q_{w\_neighbor}$	Crosstalk Penalty from Neighbors	0.5	1.4	

was compensated back to the typical QPSK constellation as shown in Fig. 7(b)[14]. Therefore, it is possible to achieve >400% SE with aggressive pre-filtering and MAP detection for the PDM-QPSK modulation format.

Table 1 summarizes the Q-factor performance for different conditions but all with 10-dB OSNR (in 1-nm RBW). With QPSK detection, single channel performance reached ∼15-dB (extrapolated from experimental measurements). However, performance degraded to 5.7 dB with all the pre- and post-filters present at 400% SE, resulting in ∼9.3-dB filtering penalty. The crosstalk penalty from neighboring channel is only 0.5 dB in this case. With MAP detection, the filtering penalty reduced to 2.2 dB. MAP detection, therefore, provided >7 dB gain compared with QPSK-only detection. Crosstalk penalty with MAP detection increased to 1.4 dB, 0.7 dB larger than with QPSK-only detection. This may be due to the fact that the $Q_{wo\_neighbor}$ was much higher with MAP detection (12.8 dB) compared with QPSK-only detection (5.7 dB).

6. 100-Gb/s transmission over 4368 km with 400% SE using pre-filtered QPSK

Figure 8 shows the received optical spectrum and OSNR with flat launch after 4368-km transmission. The original 96 DFB lasers from the 300% SE experiment were re-arranged in groups of 6 to create 25-GHz channel spacing covering the full bandwidth (with gaps). There were no more than two channels missing in a single loading gap. Similar to previous measurements, the eight ECLs were tuned to the measurement region and the corresponding DFBs were turned off during the performance measurement. We experimentally confirmed that a de-correlated 4-rail transmitter setup performed very similar to the 2-rail setup shown in Fig. 1 with 25-GHz channel spacing.

Figure 9 shows the performance of selected channels from three locations across the band with and without MAP detection after 4368-km transmission. Our 5-tap MAP detection algorithm provides >3 dB benefit over CMA alone for all channels. We also compared the performance when using a different number of taps for the MAP detection. Compared with the 5-tap MAP detection scheme, 3-tap MAP resulted in ∼2 dB lower performance[14]. The 7-tap MAP on the other hand requires much longer decoding time. To balance performance and decoding time, we therefore use 5-tap MAP for the rest of the paper. Similar to the 300% SE experiment, more EDFA power could be used to improve performance. We also found that RZ-QPSK outperformed NRZ-QPSK by ∼0.5 dB even with the aggressive pre-filtering.

7. Transmission distance limit

In our experiment, the performance for both 300% SE and 400% SE could be further improved with more EDFA power. Therefore, we also investigated the ultimate system reach with the optimum transmitter pre-emphasis for both 300% SE and 400% SE. Q-factor versus transmission distance was measured with a channel near 1550 nm. For 300% SE, we achieved ∼14000 km with Q-factor >10 dB commensurate with ∼300000 ps/nm of accumulated dispersion. For 400% SE, the transmission distance can reach ∼5000 km with Q-factor >10 dB.

Figures 11(a) and (b) show the received constellation (before MAP) after 10608 km with 300% SE and after 4368 km with 400% SE, respectively. Due to the crosstalk from neighboring channels, noise, and nonlinear phase accumulation along the transmission line, the fine structure in the transmitted constellation disappears; therefore the received constellations are not as clean as that in Fig. 7(a) (for one polarization and without two immediate neighbor channels).

8. Discussions

Figure 12 compares transmission distance versus SE for several recently published results[2−5], together with three constant distance-SE products (10, 20, 30 Mm·(bit/s)/Hz). Also shown in the figure are the lowest Q-factors reported in these papers. The SE of the results reported in Refs. [2] and [3] was 200% in both cases, but at slightly different transmission distance; the achieved distance-SE product

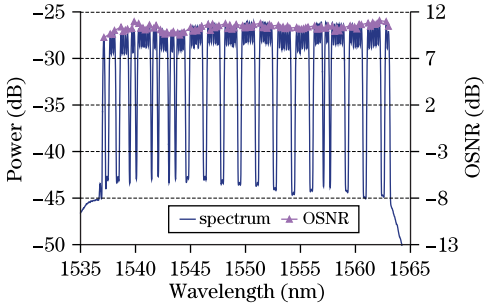

Fig. 8. Optical spectrum and OSNR (in 1-nm RBW) after 4368 km.

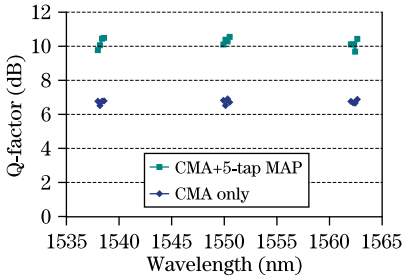

Fig. 9. Q-factor after 4368 km (400% SE) with different detection schemes.

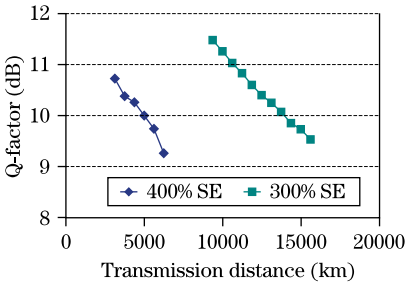

Fig. 10. Q-factor versus transmission distance for 300% and 400% SE near 1550 nm.

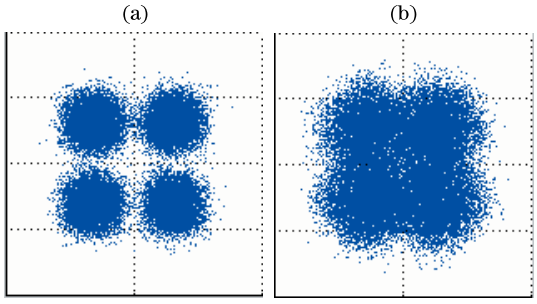

Fig. 11. Received constellation (without MAP) (a) after 10,608km with 300% SE and (b) after 4368 km with 400% SE.

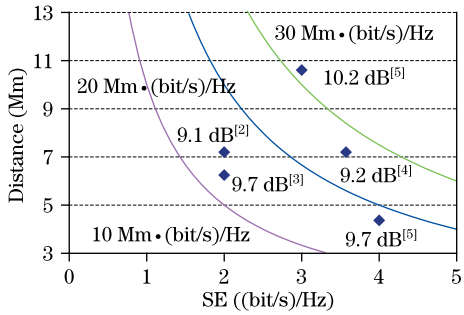

Fig. 12. Transmission distance versus SE.

was approximately 14 Mm·(bit/s)/Hz. The distance-SE product achieved in Ref. [4] was ∼26 Mm·(bit/s)/Hz at 357% SE. We report 32 Mm·(bit/s)/Hz at 300% SE, combining QPSK transmission and MAP detection, a result significantly higher than the previous distance-SE record reported in Ref. [4] using the OFDM technique. In addition, to the best of our knowledge, 400% SE also demonstrated here is the highest SE reported for the PDM-QPSK modulation format to date.

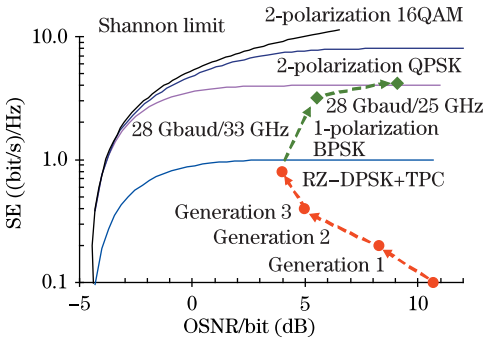

Fig. 13. Spectral efficiency versus required OSNR.

The SEs demonstrated in this paper are plotted in Fig. 13 for comparison with previous generations of terminal equipment for undersea cable systems and the SE limits for several memory-less modulation formats[10,14]. For a fair comparison, the SE definition was modified as "line bit rate/channel spacing/(1+FEC overhead)" instead of "user bit rate/channel spacing" for this paragraph only. With the modified definition, the 300% SE and 400% SE in our experiment would be 314% (112 Gb/s at 33-GHz channel spacing with 7% FEC overhead) and 419% (112 Gb/s at 25-GHz channel spacing with 7% FEC overhead), respectively.

At first glance one might conclude that this 419% result exceeds the 400% SE limit for the PDM-QPSK modulation format[15]; however, the constellation of the transmitted signal was much more complicated than that of simple 4-level QPSK shown in Fig. 7(a). By taking advantage of this complex constellation diagram, we were able to exceed the 400% SE limit of a memory-less PDM-QPSK modulation format. However, the 419% SE (achieved with the pre-filtered PDM-QPSK and MAP detection) is still far away from the Shannon limit as shown in Fig. 13.

Furthermore, we observed that this new high SE result has fundamentally changed the trend of achieved SE versus required OSNR. In previous generations of terminal equipment (Generation 1 or early 10-Gb/s OOK to RZ–DPSK+TPC, TPC: turbo product code) for undersea communication systems, the required OSNR decreased with increasing SE as we transitioned from OOK to the DPSK modulation format (while keeping the binary modulation scheme) and explored better and better FEC as shown in the lower part of the dashed line in Fig. 13. However, as we go to higher-level modulation formats, the required OSNR increases with increasing SE as shown by the upper part of the dashed line. In our current experiment, we used short spans (52 km) and larger effective area fibers (150 μm^2) to enhance OSNR.

9. Conclusions

We demonstrat 96×112-Gb/s transmission with 300% SE over 10608 km using a pre-filtered PDM-RZ-QPSK modulation format in conjunction with a MAP detection algorithm. Aggressive optical filtering reduces crosstalk from neighboring channels and induces correlation between symbols. Our MAP detection algorithm can reduce the ISI induced penalty by taking advantage of this correlation. With >3 dB MAP detection benefit, we also

demonstrated 400% SE for 112-Gb/s signals at 25-GHz channel spacing over 4368 km. Short repeater spans (52 km) and larger effective area fibers (150 μm^2) are used to maintain a high received OSNR.

References

1. G. Charlet, M. Salsi, P. Tran, M. Bertolini, H. Mardoyan, J. Renaudier, O. Bertran-Pardo, and S. Bigo, in *Proceedings of OFC/NFOEC 2009* PDPB6 (2009).
2. M. Salsi, H. Mardoyan, P. Tran, C. Koebele, E. Dutisseuil, G. Charlet, and S. Bigo, in *Proceedings of ECOC 2009* PD2.5 (2009).
3. H. Masuda, E. Yamazaki, A. Sano, T. Yoshimatsu, T. Kobayashi, E. Yoshida, Y. Miyamoto, S. Matsuoka, Y. Takatori, M. Mizoguchi, K. Okada, K. Hagimoto, T. Yamada, and S. Kamei, in *Proceedings of OFC/NFOEC 2009* PDPB5 (2009).
4. S. Chandrasekhar, X. Liu, B. Zhu, and D. W. Peckham, in *Proceedings of ECOC 2009* PD2.6 (2009).
5. J. X. Cai, Y. Cai, C. R. Davidson, D. G. Foursa, A. Lucero, O. Sinkin, W. Patterson, A. Pilipetskii, G. Mohs, and N. Bergano, in *Proceedings of OFC/NFOEC 2010* PDPB10 (2010).
6. Q. Yu, L.-S. Yan, S. Lee, Y. Xie, and A. E. Willner, J. Lightwave Technol. **21,** 1593 (2003).
7. C. Laperle, B. Villeneuve, Z. Zhang, D. McGhan, H. Sun, and M. O'Sullivan, J. Lightwave Technol. **26,** 168 (2008).
8. A. J. Viterbi and A. M. Viterbi, IEEE Trans. Inf. Theory **29,** 543 (1983).
9. Y. Cai, D. G. Foursa, C. R. Davidson, J.-X. Cai, O. Sinkin, M. Nissov, and A. Pilipetskii, in *Proceedings of OFC/NFOEC 2010* OTuE1 (2010).
10. Y. Cai, in *Proceedings of OFC/NFOEC 2008* OTuM1 (2008).
11. F. Chang, K. Onohara, and T. Mizuochi, IEEE Commun. Magazine **48,** (3) 48 (2010).
12. S. Zhang, X. Li, P. Kam, C. Yu, and J. Chen, IEEE Photon. Technol. Lett. **22,** 380 (2010).
13. N. Alic, M. Karlsson, M. Skold, O. Milenkovic, P. Andrekson, and S. Radic, J. Lightwave Technol. **28,** 1564 (2010).
14. Y. Cai, J.-X. Cai, C. R. Davidson, D. Foursa, A. Lucero, O. Sinkin, A. Pilipetskii, G. Mohs, and N. S. Bergano, in *Proceedings of ECOC 2010* We.7.C.4 (2010).
15. R.-J. Essiambre, G. Kramer, P. J. Winzer, G. J. Foschini, and B. Goebel, J. Lightwave Technol. **28,** 662 (2010).